

# Optical properties of PbS thin films chemically deposited at different temperatures

J.J. Valenzuela-Jáuregui<sup>a</sup>, R. Ramírez-Bon<sup>a,\*</sup>, A. Mendoza-Galván<sup>a</sup>, M. Sotelo-Lerma<sup>b</sup>

<sup>a</sup>Centro de Investigación y Estudios Avanzados del IPN, Unidad Querétaro, Apdo, Postal 1-798, 76001 Querétaro, Qro., Mexico

<sup>b</sup>Centro de Investigación en Polímeros y Materiales, Universidad de Sonora, Apdo, Postal 130, 83190 Hermosillo, Son., Mexico

Received 22 February 2003; received in revised form 6 June 2003; accepted 9 June 2003

## Abstract

PbS thin films were deposited on glass slide substrates using the chemical bath deposition technique. The films were obtained in a reaction bath at temperatures of 10, 15, 20, 25 and 30 °C. The structure and surface morphology of the films were studied by X-ray diffraction and by atomic force microscopy measurements. The optical properties were determined from spectroscopy measurements of ellipsometry, transmission and reflection, in the energy range of 240–840 nm. In order to analyze the ellipsometry measurements, two models for the dielectric function of the films were considered, the Bruggeman's effective medium approximation and the Lorentz oscillator expression. From this analysis, the complex dielectric function  $\varepsilon(E) = \varepsilon_1(E) + i\varepsilon_2(E)$ , thickness, roughness and void fraction of the films were examined as a function of temperature deposition. With the model obtained in the ellipsometry analysis, the optical spectra of reflection and transmission were calculated and compared with the measured spectra finding a good agreement.

© 2003 Elsevier B.V. All rights reserved.

PACS: 78.20.-e; 78.20.Ci; 78.66.Li; 81.10.Dn; 81.16.Be

Keywords: Optical properties; Ellipsometry; Deposition process; Sulfides

## 1. Introduction

PbS is a direct narrow gap semiconductor very suitable for infrared detection applications. At room temperature, its energy band gap is approximately 0.37–0.4 eV [1,2]. This material has also been used as photoresistance, diode lasers, humidity and temperature sensors, decorative coatings and solar control coatings, among others applications [3–8]. For these reasons, many research groups have an increasing interest in the development and study of this material. It is well known that the chemical bath deposition technique (CBD) is the most convenient and frequently used deposition technique to grow PbS thin films. It has been found that the properties of chemically deposited PbS thin films depend strongly on the growth conditions. Typically, this type of PbS films are deposited at room temperature and

have a well-defined grainy with somewhat loose compact structure, which has a marked influence on their photosensitivity properties [9,10].

The morphological structure characteristic of chemically deposited PbS films evidenced in surface images measured by scanning electron microscopy is also manifested on their electrical and optical properties [9–11]. On one hand, the features of the electrical transport in PbS films are those characteristics of polycrystalline materials constituted by grains and grain boundaries. On the other hand, the surface roughness and voids in the films strongly affects their reflection and transmission spectra. In the latter case, it would be expected that the differences between the optical properties of polycrystalline films and bulk PbS would arise mainly from their different morphological structure. In fact, the optical characterization of polycrystalline films can be used to obtain structural and morphological information from these materials. For example, it has been done in CdS films by measuring the complex dielectric function,

\*Corresponding author. Tel.: +52-442-2-11-99-06; fax: +52-442-2-11-99-39.

E-mail address: [rbon@ciateq.net.mx](mailto:rbon@ciateq.net.mx) (R. Ramírez-Bon).

$\varepsilon(E)$ , from spectroscopic ellipsometry measurements [12].

In this work, we investigated the influence of the deposition temperature (10–30 °C) on the optical properties and morphological structure of chemically deposited PbS films. For this, we applied spectroscopy ellipsometry to determine the complex dielectric function of the films,  $\varepsilon(E) = \varepsilon_1(E) + i\varepsilon_2(E)$  and compared the results with the optical properties of bulk PbS reported in literature. In addition, the optical spectra of transmission and reflectance of the films were measured at normal incidence. This study was complimented with X-ray diffraction (XRD) and atomic force microscopy (AFM) measurements.

## 2. Experimental details

The deposition of PbS films was done in a reactive solution prepared in a 100 ml beaker by the sequential addition of 5 ml of 0.5 M lead acetate, 5 ml of 2 M sodium hydroxide, 6 ml of 1 M thiourea and 2 ml of 1 M triethanolamine. The solution was added with deionized water to complete a total volume of 100 ml. The films were deposited on glass slide substrates. To obtain the films, three substrates were vertically immersed into the solution, supported on the wall of the beaker. The substrates were subsequently retired from the beaker at different times: 60, 90 and 120 min. Here we analyze samples obtained after 120 min of deposition. The temperature of the solution for each series growth was 10, 15, 20, 25 and 30 °C. For this, the beaker with the reactive solution was immersed in a water heating bath/circulator. The resultant films were homogeneous, well adhered to the substrate, and specularly reflecting with a varying color depending on the deposition temperature. A diffractometer Rigaku D/max-2100 was used to obtain the X-ray diffraction (XRD) patterns of the films. The two-dimensional images of the surface samples were obtained by atomic force microscopy (AFM) with a Park Scientific Instruments. The spectroscopy ellipsometry (SE) measurements were performed in the energy range of 1.5–5.0 eV (in steps of 0.05 eV), with a DH10 Uvisel system at an angle of incidence of 70°. The reflection and transmission spectra of the films were measured at room temperature under normal incidence in the spectral range of 240–840 nm (5.16–1.75 eV) using a Film Tek™ 3000 (SCI, Inc.) instrument.

## 3. Results and discussion

### 3.1. Structure and surface morphology

In Fig. 1 are shown the XRD patterns of the PbS films deposited at several temperatures, for a growth time of 120 min. The patterns display four diffraction peaks at  $2\theta$  values of approximately 26, 30, 43 and 51°,

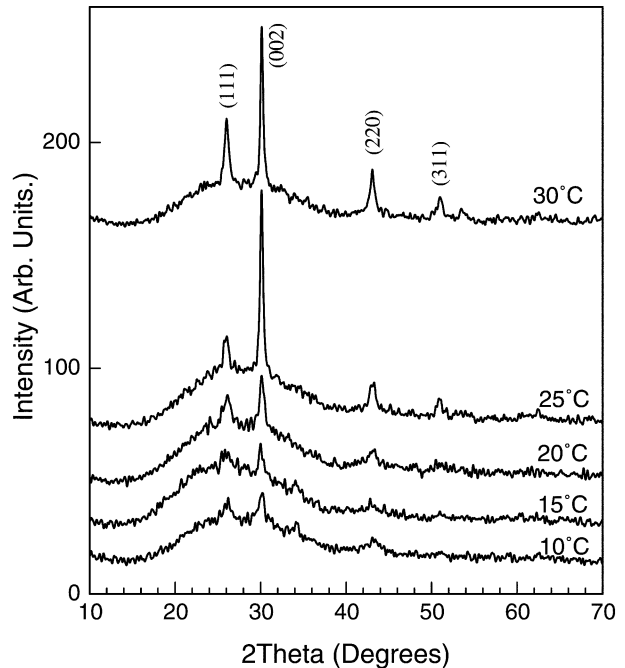


Fig. 1. X-ray diffraction patterns of PbS films deposited during 2 h at different chemical bath temperatures. The indices in the diffraction peaks correspond to the cubic PbS crystalline phase (Galena).

which correspond to the diffraction lines produced by the (111), (200), (220) and (311) crystalline planes of the PbS cubic phase (galena), respectively. It is observed a preferred orientation growth along the (200) direction. It is also observed that the intensity of the peaks increases with the temperature deposition of the films. This effect can be related to the increase of both, thickness and grain size of the PbS films with temperature. The grain size and lattice constant of the films as a function of deposition temperature were determined by fitting the more intense diffraction peaks to gaussian functions and using the Debye–Scherrer formula. The results are shown in Fig. 2. The lattice constant of the films is approximately 5.9 Å and it is not affected appreciably by the change in the temperature deposition. This lattice constant value is very similar to the bulk PbS [1], indicating that films grow on the glass substrate without stresses at the interface. However, the temperature deposition produce an increase in the grain size of the PbS films from approximately 7 to 20 nm for the films deposited at 10 and 30 °C, respectively.

The surface images in an area of  $2 \times 2 \mu\text{m}$  of the PbS films deposited at 20 and 30 °C, obtained by AFM, are shown in Fig. 3. It can be observed that the surface of the films is not very compact. The films are constituted by round shaped clusters packed together with a regular size distribution. A lot of empty spaces can be seen between these clusters. The average size of the clusters increases with temperature. The larger clusters in the

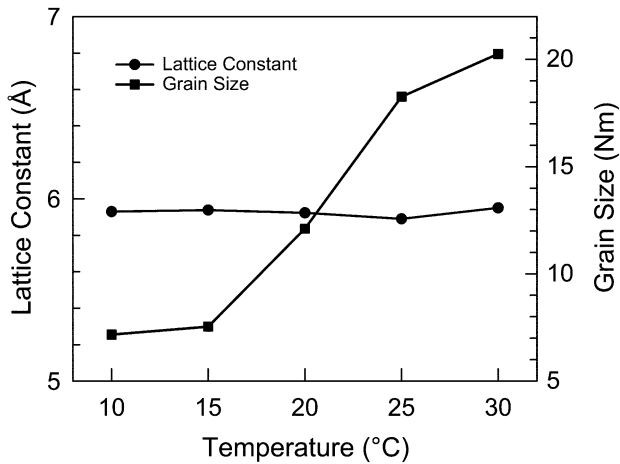


Fig. 2. Calculated lattice constant and grain size of PbS films as a function of deposition temperature.

surface of the film deposited at 30 °C exhibit clearly an aggregate structure, that is, they are composed by the small crystallites or grains. The size of these small crystallites cannot be determined from these pictures due to the image resolution. The changes in the structural and surface morphology properties of the PbS films produced by the deposition temperature can be related to the larger number of both  $\text{Pb}^{2+}$  and  $\text{S}^{2-}$  ions in the reaction solution at higher temperatures. The release of metal ions by the complexing agent is a thermal activated process and the double hidrolisation of thiourea to produce  $\text{S}^{2-}$  ions is also more effective at higher temperatures [13]. Our results show that both processes can take place in a reaction solution at temperatures as low as 10 °C.

### 3.2. Optical properties

Spectroscopic ellipsometry measurements provide the change in the polarization state that an incident linearly polarized light beam suffers when it is reflected by a surface. This change is expressed as the ratio between the complex reflection coefficients for polarization parallel  $r_p$  and perpendicular  $r_s$ , to the plane of incidence [14],

$$\rho = \frac{r_p}{r_s} = \tan\Psi \exp(i\Delta). \quad (1)$$

The spectroscopic measurements are given in terms of the ellipsometric angles  $\Psi$  and  $\Delta$  as a function of the photon energy. Thus, the construction of a physical model for the coefficients  $r_p$  and  $r_s$ , allows the determination of several parameters by fitting the calculated spectra with Eq. (1) to the experimental measurements.

Fig. 4 shows the experimental SE measurements (solid lines) for a film obtained in a bath temperature

of 30 °C. In this figure, the spectra shown with broken lines are the best fit obtained with the model described in the following paragraph.

As was shown in Fig. 1, for this film clearly the diffraction lines of PbS can be seen, and the film is composed of an aggregate structure revealed in the AFM image of Fig. 3b. Such structure suggests that the film can be appropriately described as a mixture of PbS and voids. In this case, the Bruggeman's effective medium approximation (EMA) can be used to represent the optical response of the film. For a two-phase system, the EMA provides an effective dielectric function  $\varepsilon$  given by [14],

$$f_a \frac{\varepsilon - \varepsilon_a}{\varepsilon + 2\varepsilon_a} + (1 - f_a) \frac{\varepsilon - \varepsilon_b}{\varepsilon + 2\varepsilon_b} = 0, \quad (2)$$

where  $\varepsilon_a$  and  $\varepsilon_b$  are the dielectric function of the constituents phases,  $f_a$  and  $1 - f_a$  are the volume frac-

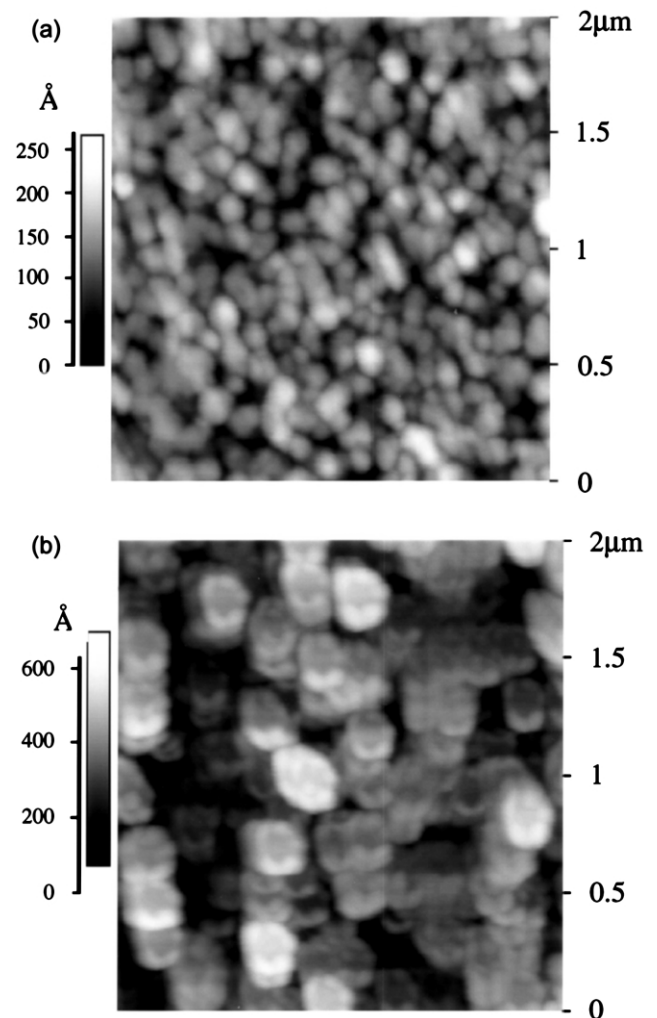


Fig. 3. Two-dimensional AFM surface images of the films deposited at temperatures of (a) 20 °C and (b) 30 °C. The area in both images is  $2 \times 2 \mu\text{m}$ .

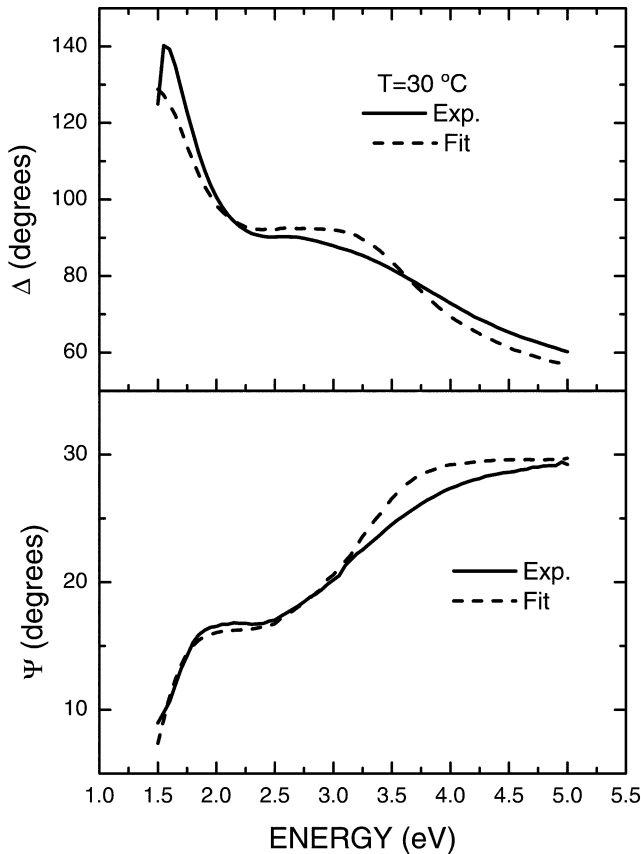


Fig. 4. Experimental ellipsometry spectra (solid line) and best fit (dashed line) for the film deposited at 30 °C. The effective dielectric function for the film was considered as a mixture of voids and PbS, using the Bruggeman's approximation (EMA).

tions occupied by the phase *a* and *b*, respectively. In the present case, for phase *a*, it can be used as the dielectric function reported in the literature for PbS single crystal [2], and for phase *b* it is used as that of voids ( $\epsilon_b = 1$ ). However, to obtain the fit shown in Fig. 4, the film was considered to be composed by two layers with different void volume fractions, where the outer layer represents the surface roughness of the film. From the fitting procedure, the thickness and void volume fraction of each layer were obtained. The results show that this sample can be described by an external layer (surface roughness) with 23.5-nm thick and 50% of voids, and a denser layer attached to the substrate with a thickness

of 130 nm and 27% of voids. A similar structure has been used successfully to describe the SE measurements for chemically bath deposited CdS films [12].

Although the two-layer-EMA model described in the above paragraph gives an acceptable description of the SE measurements for the considered sample, it was found that such model does not work for films grown at other temperatures than 30 °C. In fact, in Fig. 4, some differences can be noticed between the experimental and fitted spectra. For these reasons, it was considered to use an analytical representation for the dielectric function of our polycrystalline PbS films. Because the energy range of the SE measurements is above of the energy gap of PbS, the optical response of the material can be represented by the Lorentz harmonic oscillator (LHO) expression [14], which can be written as:

$$\epsilon(E) = \epsilon_{\infty} \left( 1 + \sum_{j=1}^3 \frac{A_j^2}{E_j^2 - E^2 - iE\Gamma_j} \right), \quad (3)$$

where  $\epsilon_{\infty}$  is the high-energy dielectric constant,  $A_j$ ,  $E_j$  and  $\Gamma_j$  are the amplitude, central energy and broadening parameter of the *j*-th oscillator, respectively. For PbS, three electronic transitions above of the energy gap have been reported at the energies of  $E_1 = 1.94$ ,  $E_2 = 3.14$  and  $E_3 = 5.27$  eV [2], and have been represented with a similar expression as Eq. (3). Fixing the values of  $\epsilon_{\infty} = 1.7$  and  $E_j$  in Eq. (3), and fitting the remaining parameters  $A_j$  and  $\Gamma_j$ , the complex dielectric function of PbS single crystal can be described in our measurement energy range (1.5–5.0 eV), with the parameters listed in Table 1.

Fig. 5 shows the SE measured spectra with solid symbols for films deposited at temperatures of 15, 20 and 30 °C. For clarity, only some experimental points are shown. In this figure, the continuous lines are the fitted spectra, which were obtained considering the structure of the PbS films as composed of a homogeneous layer with dielectric function given by Eq. (3) and a surface layer representing surface roughness, where this top layer is described by the EMA expression, Eq. (2), with 50% voids and 50% of material. Similar results were obtained for samples deposited at the other temperatures. The fitting parameters for the LHO expression are listed in Table 1. It must be mentioned that the  $\epsilon_{\infty} = 1.7$  and  $E_3$  values were fixed in the fitting proce-

Table 1  
Parameters of the LHO model for PbS samples

Sample	$E_1$ (eV)	$A_1$	$\Gamma_1$	$E_2$ (eV)	$A_2$	$\Gamma_2$	$E_3$ (eV)	$A_3$	$\Gamma_3$
15 °C	2.36	1.24	0.92	3.68	5.07	1.55	5.27	8.74	4.17
20 °C	2.23	1.04	0.61	3.47	5.26	1.51	5.27	8.15	4.14
30 °C	2.19	1.21	0.67	3.25	6.12	1.65	5.27	7.7	6.16
PbS single crystal	1.94	2.53	0.87	3.14	7.87	1.35	5.27	4.81	2.09

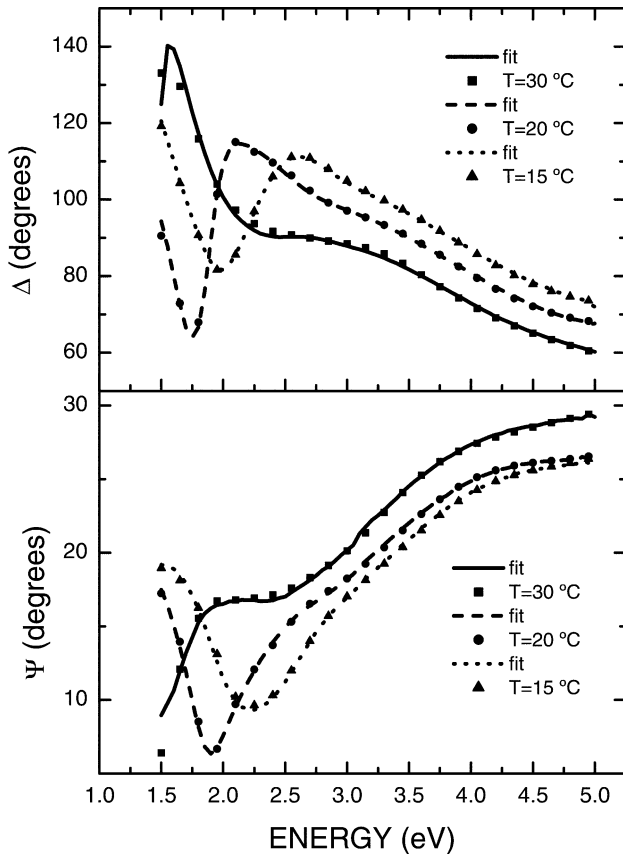


Fig. 5. Experimental (symbols) and best-fit (lines) ellipsometry spectra for films deposited at the three indicate temperatures. These fits were obtained with the Lorentz harmonic oscillator model (LHO) for the dielectric function of the films.

ture. For comparison, the parameters corresponding to bulk PbS [2] are also listed in this table. It can be seen that the  $E_1$  and  $E_2$  values are shifted to high-energy values respect to those of the single crystal, however, as the deposition temperature increases there is a trend to attain the single crystal values.

The film thickness ( $t$ ) and average roughness ( $r$ ) were also determined from the fitting procedure. The  $t$  and  $r$  values obtained are shown in Fig. 6 as a function of deposition temperature. As was inferred from XRD measurements, it can be noticed in Fig. 6 that the quantity of deposited material in the films increases with temperature deposition. The thickness of the films runs from 55 to 143 nm for the films deposited at 10 °C and 30 °C, respectively. The results for the roughness of the films surface show low values between 11 and 24 nm, with a weak dependence on the deposition temperature. The average roughness decreases from 23 nm for the film deposited at 10 °C to approximately 11 nm for the film deposited at 15 °C, then, it increases up to 24 nm for the film deposited at 30 °C.

The complex dielectric function of PbS films (homogeneous layer) deposited at temperatures of 15, 20 and

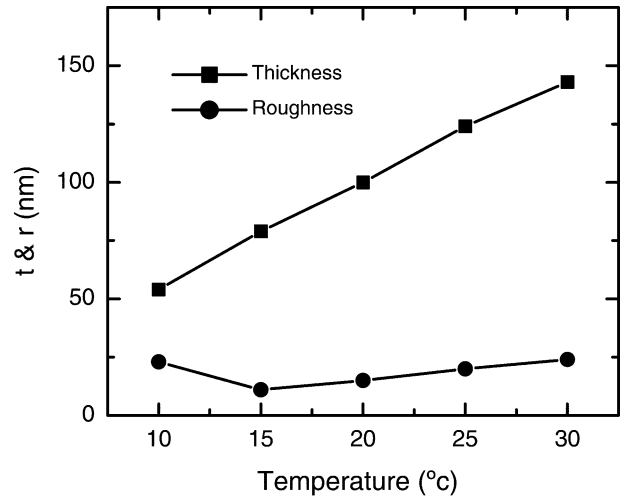


Fig. 6. Thickness and roughness values as a function of deposition temperature, obtained from fitting the ellipsometry spectra as was shown in Fig. 5.

30 °C are shown in Fig. 7a. The line shape of these spectra agrees with that obtained from PbS single crystal. Clearly in the  $\epsilon_2$  spectra are shown the two-electronic transitions of PbS in the measurement energy range; one

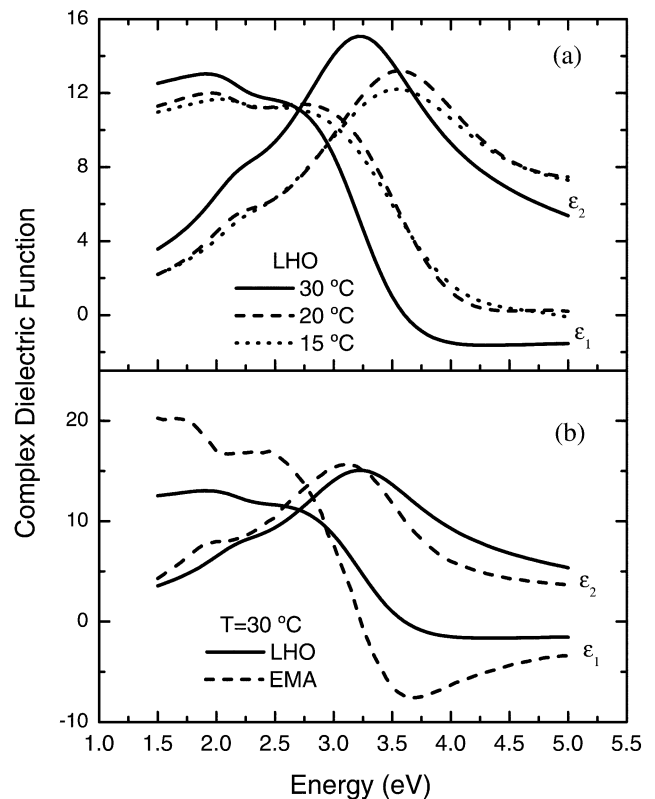


Fig. 7. (a) Effect of the deposition temperature on the complex dielectric function for PbS films. (b) Comparison between the complex dielectric functions obtained with the EMA model (fit in Fig. 4) and with the LHO model (fit in Fig. 5), for the film deposited at 30 °C.

the shoulder at approximately 2.19–2.36 eV, and the other, the maximum at approximately 3.25–3.55 eV, which correspond to the  $E_1$  and  $E_2$  critical points, respectively. The energy position of these transitions depends on deposition temperature. The maximum values  $\varepsilon_2 = 15.06$ , 13.2 and 12.21 at energies of 3.25, 3.55 and 3.55 eV. In single crystals, the value is of 26.4 in the  $E_2$  peak at 3.14 eV. The shift could be attributed to the small grain size, which was smaller than 20 nm, as obtained from XRD data analysis and shown in Fig. 2.

However, as was shown in Fig. 4, the SE spectra for the film deposited at 30 °C were fitted with the EMA model, the effective dielectric function obtained in this case, is shown in Fig. 7b where it is compared with the dielectric function obtained with the LHO model. Clearly both models exhibit similar features of the  $\varepsilon$  spectra. In particular, the imaginary part,  $\varepsilon_2$  spectra show similar heights, but the LHO spectrum is shifted to high energies. From this comparison it can be concluded that the void fraction for this film is that obtained with the EMA model being approximately of 27%. As is shown in Fig. 7a, the  $\varepsilon_2$  spectra of the films deposited at lower temperatures than 30 °C, have lower values indicating an increasing void fraction as the temperature of deposition decreases. The estimated void volume fraction for the film deposited at 10 °C is approximately 42%.

Fig. 8 shows the experimental transmission ( $T$ ) and reflection ( $R$ ) spectra (solid lines) for films deposited at temperatures of 10, 20 and 30 °C. The broken lines in Fig. 8 correspond to the spectra calculated with the model used to describe the SE measurements. As can be seen, the experimental and calculated spectra of  $R$  and  $T$  agree quite well. In Fig. 8a, as the deposition temperature increases the transparency window decreases, because to the increasing thickness with temperature. In the case of reflectance spectra, Fig. 8b, the thickness effect is noticed in the long wavelength portion of the spectra, where interference effects take place. This is accounted for wavelengths longer than 600 nm for films deposited at 20 and 30 °C, and for  $\lambda > 450$  nm in the thinnest film which was deposited at 10 °C. For wavelengths in the range of 350–600 nm, the reflectance is more or less constant with values of approximately 30% and 25% for the films deposited at 20 °C and 30 °C, respectively. At wavelengths approximately 350 nm, where the films are absorbing, it is expected that the reflectance spectra reach the maximum value of approximately 60% [2], near to the  $E_2$  critical point. However, at such wavelength the films exhibit rather low  $R$ -values, which are explained by the presence of surface roughness. It is known that the surface roughness has a great effect on the optical measurements, mainly at wavelengths (energies) close to electronic transitions [15]. Hence, the film deposited at 20 °C shows higher  $R$ -values than films deposited at 10 and 30 °C, because to the difference in surface roughness, as was shown in

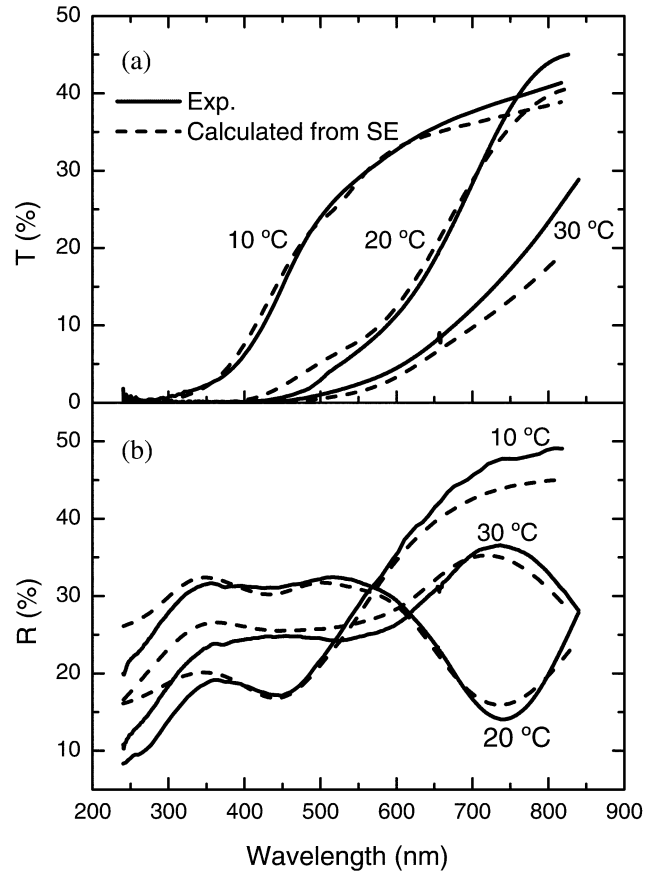


Fig. 8. Experimental (solid lines) transmittance (a) and reflectance (b) spectra as a function of the deposition temperature. The calculated  $R$  and  $T$  spectra (dashed lines) were obtained using the LHO dielectric function, the thickness and roughness values obtained from the fit of the ellipsometry spectra.

Fig. 6. Thus, the color displayed by the films under reflected light results from a combined effect: one, the film thickness, which controls the red component and the other, surface roughness, which affects the violet–blue component.

#### 4. Conclusions

The optical properties of chemically deposited PbS films, at different temperatures, were studied by means of spectroscopic measurements of ellipsometry, transmission and reflection. From the data analysis of the ellipsometry spectra, the complex dielectric function, thickness and roughness were obtained. It was found that the  $\varepsilon$  spectra of these films differ from that of single crystal, in both absolute values and energy position of the critical points. Such differences can be explained in terms of the microstructure displayed by the films, as revealed in the AFM images. The low values of  $\varepsilon$  for the films, are due to the empty space between the aggregates that comprising the films. The

estimated void volume fraction with the effective medium analysis, give values of 42 and 27% for films deposited at 10 °C and 30 °C, respectively. By his side, the shift of the critical points can be related to the smallness of the crystallites forming the aggregates.

### Acknowledgments

This work was financially supported by CONACyT from México (Projects No. 34514-U and 31303-U). We acknowledge the helpful technical assistance of M.A. Hernández-Landaverde and J.E. Urbina-Álvarez.

### References

- [1] J.I. Pankove, *Optical Processes in Semiconductors*, Dover Publications Inc, New York, 1971.
- [2] H. Kanazawa, S. Adachi, *J. Appl. Phys.* 83 (1998) 5997.
- [3] I. Pop, C. Nascu, V. Ionescu, E. Indrea, I. Bratu, *Thin Solid Films* 307 (1997) 240.
- [4] C. Nascu, V. Vomit, I. Pop, V. Ionescu, R. Grecu, *Mater. Sci. Eng. B* 841 (1996) 235.
- [5] P.K. Nair, M.T.S. Nair, A. Fernández, M. Ocampo, *J. Phys. D: Appl. Phys.* 22 (1989) 829.
- [6] P.K. Nair, V.M. García, A.B. Hernandez, M.T.S. Nair, *J. Phys. D: Appl. Phys.* 24 (1991) 1466–1472.
- [7] N.I. Fainer, M.L. Kosinova, Yu.M. Romyantsev, E.G. Salman, F.A. Kuznetsov, *Thin Solid Films* 280 (1996) 16.
- [8] P.K. Nair, M.T.S. Nair, *J. Phys. D: Appl. Phys.* 23 (1990) 150.
- [9] G.H. Blount, P.J. Schreiber, D.K. Smith, R.T. Yamada, *J. Appl. Phys.* 44 (1973) 978.
- [10] G.P. Kothiyal, B. Ghosh, R.Y. Deshpande, *J. Phys. D: Appl. Phys.* 13 (1980) 869.
- [11] M.B. Ortuño-López, J.J. Valenzuela-Jáuregui, R. Ramírez-Bon, E. Prokhorov, J. González-Hernández, *J. Phys. Chem. Solids* 63 (2002) 665.
- [12] A. Mendoza-Galván, G. Martínez, R. Lozada-Morales, *J. Appl. Phys.* 80 (1996) 3333.
- [13] K.L. Chopra, S. Ranjan Das, *Thin Film Solar Cells*, Plenum Press, New York and London, 1983, p. 229.
- [14] G.E. Jellison Jr, *Thin Solid Films* 234 (1993) 416.
- [15] C. Pickering, in: P. Halevi (Ed.), *Photonic Probes of Surfaces*, Elsevier, Amsterdam, 1995, p. 1.